A New Model of Patient Tumor-Derived Breast Cancer Xenografts for Preclinical Assays

Elisabetta Marangoni,[1] Anne Vincent-Salomon,[3] Nathalie Auger,[1] Armelle Degeorges,[2] Franck Assayag,[1] Patricia de Cremoux,[2] Ludmilla de Plater,[1] Charlotte Guyader,[1] Gonzague De Pinieux,[6] Jean-Gabriel Judde,[1] Magali Rebucci,[1] Carine Tran-Perennou,[2] Xavier Sastre-Garau,[3] Brigitte Sigal-Zafrani,[3] Olivier Delattre,[5] Véronique Diéras,[4] and Marie-France Poupon[1]

Abstract

Purpose: To establish a panel of human breast cancer (HBC) xenografts in immunodeficient mice suitable for pharmacologic preclinical assays.

Experimental Design: 200 samples of HBCs were grafted into Swiss nude mice. Twenty-five transplantable xenografts were established (12.5%). Their characterization included histology, p53 status, genetic analysis by array comparative genomic hybridization, gene expression by Western blotting, and quantitative reverse transcription-PCR. Biological profiles of nine xenografts were compared with those of the corresponding patient's tumor. Chemosensitivities of 17 xenografts to a combination of Adriamycin and cyclophosphamide (AC), docetaxel, trastuzumab, and Degarelix were evaluated.

Results: Almost all patient tumors established as xenografts displayed an aggressive phenotype, i.e., high-grade, triple-negative status. The histology of the xenografts recapitulated the features of the original tumors. Mutation of p53 and inactivation of Rb and PTEN proteins were found in 83%, 30%, and 42% of HBC xenografts, respectively. Two HBCx had an ERBB2 (HER2) amplification. Large variations were observed in the expression of HER family receptors and in genomic profiles. Genomic alterations were close to those of original samples in paired tumors. Three xenografts formed lung metastases. A total of 15 of the 17 HBCx (88%) responded to AC, and 8 (47%) responded to docetaxel. One ERBB2-amplified xenograft responded to trastuzumab, whereas the other did not. The drug response of HBC xenografts was concordant with that of the patient's tumor in five of seven analyzable cases.

Conclusions: This panel of breast cancer xenografts includes 15 triple-negative, one ER positive and 2 ERBB2 positive. This panel represents a useful preclinical tool for testing new agents and protocols and for further exploration of the biological basis of drug responses.

Breast cancer is one of the most frequently diagnosed types of cancer in women and a leading cause of cancer-related death in women. The incidence of breast cancer has increased by two-thirds over the last 15 years. However, mortality has decreased by one-third due to the earlier detection of breast cancer and increasing use of systemic therapies. Recently, new chemotherapy agents and molecular targeted therapies, such as trastuzumab, have provided a real hope of decreasing breast cancer mortality. However, despite appropriate adjuvant systemic therapy, up to 30% of patients will relapse. The vast majority of deaths are caused by recurrent metastatic disease. To date, patients relapsing will frequently have received multiple therapies in the adjuvant setting (anthracycline-taxane–based chemotherapy, hormonotherapy, and trastuzumab in case of ERBB2 amplification). Therefore, it is clear that novel compounds are required in the metastatic setting. Considering the numerous compounds produced by pharmaceutical companies, we need new tools to speed up clinical development and to take into account the heterogeneity of the disease. Preclinical models are one potential solution. A preclinical screening step in drug development must predict not only the antitumoral activity of new compounds, but also in which tumor type or subtype the compound will be effective. The preclinical models presently used are not predictive enough for such purposes. Most of the existing *in vivo* models for preclinical assays of anticancer drugs are based on a limited number of cell lines previously isolated from human tumors and selected through culture before their implantation into immunodeficient animals. Cancer cell xenografts have been widely used due to their well-characterized features, the possibility of interlaboratory comparison, and reproducibility. However, they do not reflect breast cancer heterogeneity, and

Authors' Affiliations: [1]U612 Institut National de la Sante et de la Recherche Medicale, Pharmacologie Préclinique Antitumorale, [2]Unité de Pharmacologie, [3]Service de Pathologie, [4]Medical Oncology, [5]U830 Institut National de la Sante et de la Recherche Medicale, and [6]Institut Curie, Paris Anatomie et Cytologie Pathologique, Hôpital Trousseau, Tours, France

Received 1/12/07; revised 4/5/07; accepted 4/20/07.

The costs of publication of this article were defrayed in part by the payment of page charges. This article must therefore be hereby marked *advertisement* in accordance with 18 U.S.C. Section 1734 solely to indicate this fact.

Requests for reprints: Marie-France Poupon, Pharmacologie Antitumorale Préclinique, Transfert Department, Institut Curie, 26 rue d'Ulm, 75005 Paris, France. Phone: 331-423-46667; Fax: 331-423-46674; E-mail: Marie-France.Poupon@curie.fr.

doi:10.1158/1078-0432.CCR-07-0078

their predictive value may be weak. New models of preclinical evaluation must be designed and validated to conduct drug development. Better preclinical models can be obtained by reducing the disparity between the original patient tumor and the *in vivo* models. For these reasons, there has recently been renewed interest in preclinical assays based on tumor xenografts obtained by the engraftment of tumor samples directly transplanted into animals. Contrasting with cell line–derived xenografts, tumor xenografts maintain the cell differentiation and morphology, the architecture, and molecular signatures of the original patient tumors (1). Vasculature, stroma, central necrosis, and peripheral growth occur in tumor-bearing mice in a way that is similar to that of the patient's tumor. Cell line–derived xenografts usually show a monomorphic, poorly differentiated histology and lack of tissue organization, namely, the adenocarcinoma architecture. Moreover, a high correlation between drug response of tumor xenografts was found with the corresponding original tumors, with a positive prediction of 90%, which is much higher that the predictive value found with *in vitro* models, as reported by Fiebig's group (2), and observed by us.[7] However, few models of breast cancer xenografts are currently available; hence, the well-known diversity of these cancers is not represented in existing preclinical models. For some human carcinomas, such as non–small cell lung cancers or colorectal cancers, the establishment of human tumor xenografts in nude mice has been achievable with a success rate of more than 50%.[7] Conversely, breast tumor xenografts derived from patient biopsies are particularly difficult to obtain, as reported by several teams (3). Breast tumors have one of the lowest tumor take rates in immunodeficient mice. Moreover, breast cancers are known for their pathologic and biological heterogeneity, with considerable differences in histology, genetics, and sensitivity to chemo- and targeted therapies. Therefore, a preclinical model of breast cancer must be constituted of a consistent series of xenografts that recapitulate this heterogeneity. Such a model of breast cancers could identify new therapeutic targets, validate the *in vitro* based screening of new compounds and potentially guide the choice of therapy for a given tumor. Furthermore, such models will allow studies of biological mechanisms of sensitivity and/or resistance. To achieve these aims, it is critical that breast cancer xenografts conserve the characteristics of the original tumor. Here, we describe a new panel of breast tumor models, established as tumor xenografts stably growing in immunodeficient mice. The direct implantation of patient tumor fragments into the s.c. interscapular fat pad of mice was chosen as we have observed that this site was more favorable than the orthotopic site for tumor take and growth. Institute Curie's colony of Swiss nude mice provides animals with a relative high tumor take frequency, which seems to be equivalent to that of BALB/c mice or severe combined immunodeficiency mice. Histologic and biological characterization of these xenografts showed their close similarity to the original cancers. Pairing of patient tumors with their corresponding xenograft allowed us to accurately compare histology, genetic parameters, and gene and protein expression of hormone and growth factor receptors. Chemosensitivity screening of xenografts was compared with the response of patients' tumors to the same chemotherapies, in few available cases. In summary, we report here the establishment and characterization of a series of human breast transplantable xenografts in nude mice with regard to their histology, biological profile, and response to standard treatments.

Materials and Methods

Animals and establishment of tumor xenografts. Breast cancer fragments were obtained from patients at the time of surgery, with informed written patient consent. Fragments of 30 to 60 mm^3 were grafted s.c. into the interscapular fat pad of 8- to 12-week-old female Swiss nude mice, under avertin anesthesia. Mice were maintained in specific pathogen-free animal housing (Institut Curie) and received estrogen (17 mg/mL) diluted in drinking water. Xenografts appeared at the graft site 2 to 8 months after grafting. They were subsequently transplanted from mouse to mouse and stocked frozen in DMSO-fetal calf serum (FCS) solution or frozen dried in nitrogen for further studies and a fragment fixed in phosphate buffered saline (PBS) 10% formol for histologic studies. The experimental protocol was done according to French regulations.

Histology of original tumors and xenografts. The morphology of patients' tumor tissues was compared with their corresponding xenografts using paraffin-embedded sections and standard protocols (4). Tumors were removed from mice and immediately fixed in a 10% formol solution for immunohistologic analysis.

Compounds and therapeutic assays. Adriamycin, 2 mg/kg (Doxorubicin, Teva Pharmaceuticals), and cyclophosphamide, 100 mg/kg (Endoxan, Baxter), diluted in 0.9% NaCl and docetaxel, 20 mg/kg (Taxotere, Sanofi-Aventis), diluted in its specific excipient, were given by the i.p. route at 3-week intervals. Trastuzumab (Herceptin, Roche) was diluted in 0.9% NaCl and given i.p. weekly at a dose of 10 mg/kg. Degarelix (Ferring) was diluted in 5% mannitol and injected s.c. monthly at a dose of 10 mg/kg. Human breast cancer (HBC) xenografts were transplanted into female 8-week-old Swiss nude mice, as described above, one tumor being transplanted into eight recipients. When tumors reached a volume of 60 to 200 mm^3, mice were individually identified and randomly assigned to the control or treated groups (8 to 12 mice per group), and the treatments were started. Tumor growth was evaluated by measurement of two perpendicular diameters of tumors with a caliper twice to thrice per week. Individual tumor volumes were calculated as $V = a \times b^2/2$, a being the largest diameter, b the smallest. For each tumor, Vs were reported to the initial volume as relative tumor volume (RTV). Means (and SE) of RTV in the same treatment group were calculated, and growth curves were established as a function of time. Optimal tumor growth inhibition (TGI) of treated tumors versus controls was calculated as the ratio of the mean RTV in treated group to the mean RTV in the control group at the same time. Statistical significance of TGI was calculated by the paired Student's t test by comparing the individual RTVs in the T and C groups. T/C tumor growth delays (GD) were calculated as the time required to reach the same RTV in the treated group T and the control group C (usually at a RTV of 4). Four categories of HBC responders were defined: (a) high responders (HR), in which the treatment induced complete regressions (the established tumors being no longer palpable after treatment); (b) the responders (R), in which TGI and T/C GD was superior to 50% and 2-fold, respectively; (c) low responders, with TGI and T/C GD comprised between 40% and 50% and 1.5 and 2, respectively; and (d) the nonresponders (No in the tables), in which the growth parameters were not significantly altered by the treatment. Mice were ethically sacrificed when the tumor volume reached 3,500 mm^3.

Biological profile of tumors and xenografts. p53 mutations were detected in xenografts by a functional assay that tests the transcriptional competence of human p53 expressed in yeast (5, 6).

Detection of Rb, AKT, P-AKT, vascular endothelial growth factor, and PTEN proteins by Western blotting. Frozen tumors were ground in

[7] Unpublished data.

liquid nitrogen and the resulting powder was incubated in lysis buffer [50 mmol/L Tris-HCl (pH 7.9), 120 mmol/L NaCl, 1% Nonidet P40, 1 mmol/L EDTA, 5 mmol/L NaF, 1 mmol/L Na_3VO_4, 0.04 mmol/L 4-(2-aminoethyl)-benzene-sulfonyl fluoride (AEBSF) and a commercial protease inhibitor mixture (Roche Applied Science) for 2 h at 4°C and cleared by centrifugation. Proteins were resolved on a reducing 4% to 12% SDS polyacrylamide gel and transferred into polyvinylidene diflouride membranes. The transferred membranes were blocked overnight at 4°C in 5% nonfat dried milk in phosphate-buffered Tween (Bio-Rad) and incubated at room temperature for 3 h with the appropriate primary antibodies, HER2 (Zymed), Rb (PharMingen), P-AKT (Cell Signaling Technology), PTEN (sc-7974, Santa Cruz Biotechnology), vascular endothelial growth factor (VEGF; sc-152, Santa Cruz Biotechnology). Membranes were washed thrice with 5% nonfat dried milk for 10 min and incubated with horseradish peroxidase–coupled isotype-specific secondary antibodies in PBS for 1 h at room temperature. The immune complexes were detected by an enhanced chemiluminescence detection system (Amersham Biosciences) and quantified using Image Gauge software.

Detection of ERα, ERβ, PR, HER1, HER2, HER3, HER4, Ki67, and cyclin E1 and E2, MDR1, MRP1, and MRP5 by quantitative RT-PCR. Total RNA extraction and cDNA synthesis were done as previously described from 1 μg total RNA (7). ERα, ERβ, PR, HER1 to HER4, Ki67, and cyclin E1 and E2, MDR1, MRP1, and MRP5 transcripts were quantified using real-time quantitative reverse transcription-PCR (RT-PCR) assays. The nucleotide and probe sequences and the conditions of PCR have been previously described (8). Results were expressed as *N*-fold differences in target gene expression relative to a reference gene defined as "*N* target" and was determined as follows: $N \text{ target} = E_{\text{target}}^{(Ct \text{ calibrator} - Ct \text{ sample})} / E_{\text{reference gene}}^{(Ct \text{ calibrator} - Ct \text{ sample})}$, where E is the efficiency of PCR measured using the slope of the calibration curve, and C_t is the cycle threshold.

Array-based comparative genomic hybridization (CGH). A genome-wide resource of 3,342 fluorescence *in situ* hybridization–mapped, sequenced BAC and PAC clones verified for gene and marker content were represented as immobilized DNA targets on glass slides for array-based CGH analysis, allowing a mean resolution of 1 Mb all along the genome. Each clone was spotted in triplicate on a slide with an aminosilane coating (Corning UltraGAPS, NH3+, Life Sciences) with the Microgrid TAS BioRobotics spotter. These slides were prepared by the Institut National de la Sante et de la Recherche Medicale Unit U830. After extraction, 1.5 μg of each test and control DNA sample was digested with *Dpn*II enzyme (Ozyme) and purified with a QIAquick PCR purification kit (Qiagen). They were then labeled by random priming using a Bioprime DNA labeling kit (Invitrogen) with the appropriate cyanine dye (Cy3 or Cy5; Perkin-Elmer). The control and test DNAs were coprecipitated with Cot-1 DNA (Invitrogen), denatured, and resuspended in hybridization buffer (50% formamide). Competitive cohybridization was done on CGH-array slides preblocked by succinic anhydride/*N*-methyl-2-pyrrolidinone/borate buffer. After a 24-h hybridization, slides were washed with SDS and saline citrate, dried, and scanned using a 4000B scan (Axon). Image analysis was done with Genepix 5.1 software (Axon) and processed using a software developed at the Curie Institute. Any BAC with less than two replicates flagged for not fulfilling qualitative spot criteria was excluded. A ratio below 0.8 was considered as a loss, a ratio higher than 1.2 was considered as a gain, and a ratio higher than 1.5 was considered as amplification (9).

Results

Samples of 200 breast adenocarcinomas (primaries and/or metastases) were obtained during surgery and implanted s.c. into the interscapular fat pad of athymic mice. Twenty-five gave growing tumors at the site of graft, and 22 were maintained by serial transplantation up to the third passage.

Clinical characteristics of the patients. The clinical characteristics are presented in Table 1. The median age was 60 (range, 32-93). Tumor size was superior to 10 mm in 95% of patients, 35% of samples coming from large (>30 mm) tumors. Both invasive lobular carcinoma (ILC) and invasive ductal carcinoma (IDC) histology was represented, 14.2% and 85.8%, respectively. Few HBC were of low grade, a majority of tumors were of grade II or III, and 70% were estrogen-receptor positive. Axillary lymph nodes were positive in two-thirds of cases. Tumor samples came from primary or distant metastases in 83% and 17%, respectively. Almost all patients (84%) did not receive any treatment before surgery, while 16% were treated either with chemotherapy, radiotherapy, or both.

Parameters related with HBC transplantation. The engraftment rate was higher when tumor tissues came from metastatic sites, as compared with primary tumors (24% versus 15%; Table 1). Tumor take of ductal carcinomas was higher than that of lobular carcinomas, 18% versus 8%, respectively, as the fraction of metastatic tumors was higher in ILC than in IDC (28% versus 15%). Tumor take of high-grade tumors (grades II and III) was superior to that of low-grade tumors. Estrogen receptor–negative tumors had a 37% tumor take versus 4% for ER-positive tumors; several ER-positive xenografts were lost after the early (first to third) transplantation passages, decreasing the tumor take rate to <1%. Neither tumor size nor lymph node involvement influenced the tumor take.

Histology of xenografts and comparison with patient tumors. The comparison between the histology of the original tumors and

Table 1. Clinical characteristics of patients, distribution by class, and corresponding frequency of tumor take in mice

Patient characteristics			Tumor take, *n* (%)*
Parameter	**Class**	**Frequency in the population (%)**	
Age	<48	11.2	3 (1/30)
	<48 and >55	28	13 (6/45)
	>55	60.8	20 (23/118)
Grade	1	19	3 (1/34)
	2	41	11 (8/75)
	3	40	30 (22/74) †
Histology	ILC	14.2	8 (2/25)
	IDC ‡	85.8	18 (28/152)
Estrogen receptor	+	70	4 (5/125)
	-	30	37 (19/52) †
Axillary lymph-node	+	59.8	16 (23/134)
	-	40.2	16 (10/64)
Tumor size (mm)	<10	5	33 (2/6)
	>10 and <30	48	13 (8/61)
	>30	47	22 (13/62)
Site of origin	Primary	83	15 (25/164)
	Metastasis§	17	24 (8/34)

*Tumor take at the first passage.
† The frequency of tumor take is statistically different between grade 3 and 1 or 2 and between ER-positive and ER-negative tumors, as calculated with the χ^2 test.
‡ Including subtypes such as mucin-producing carcinomas, basal-like carcinomas, and medullary carcinomas.
§ Including the tumor tissue coming from axillary lymph node and omentum metastasis; ILC invasive lobular carcinoma, IDC, invasive ductal carcinoma.

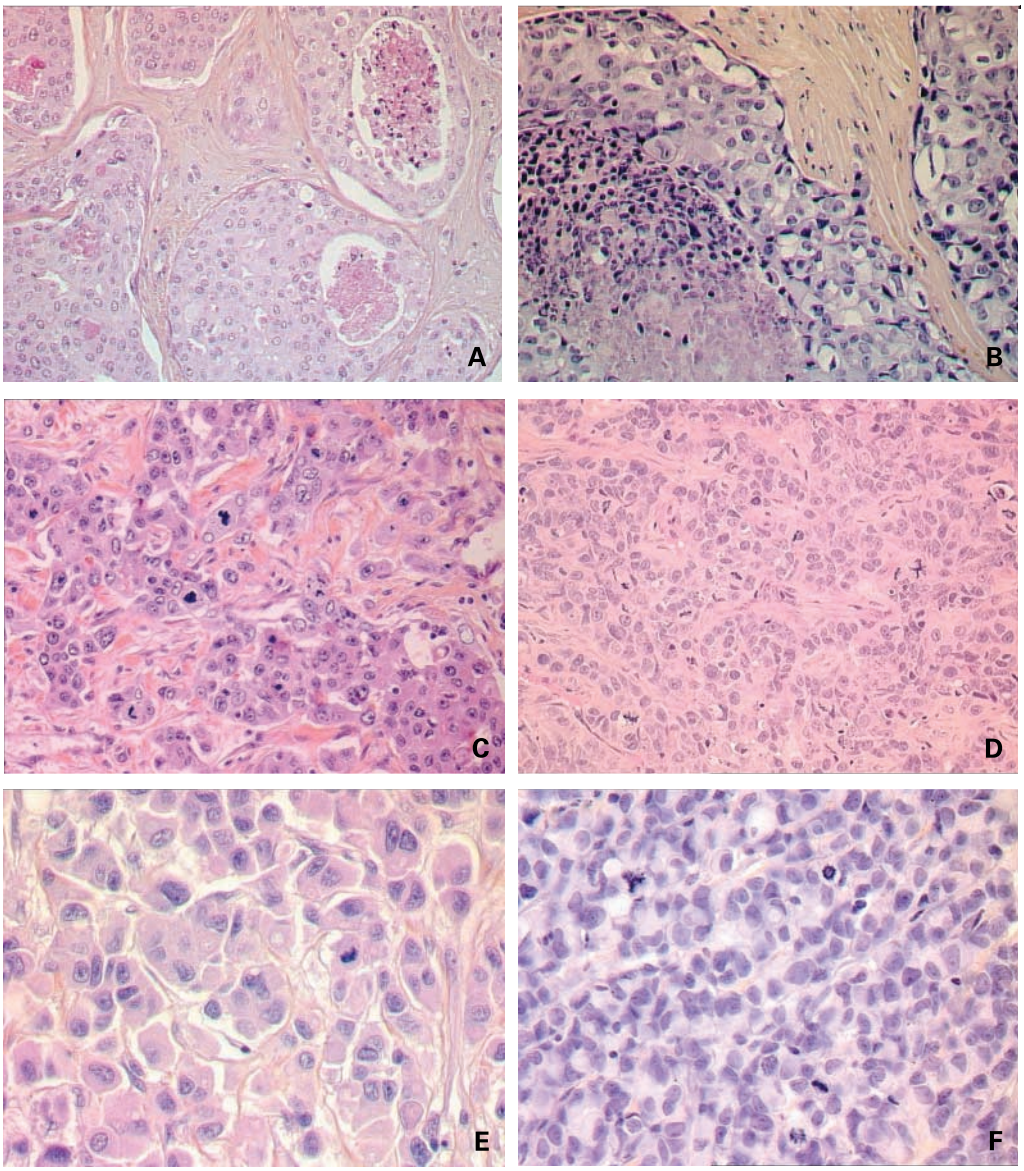

Fig. 1. Histologic features of patient breast cancers and their corresponding xenograft. HBC-13 (*A*), HBCx-13A (*B*), HBC-4 (*C*), HBCx-4 (*D*), HBC-19 (*E*), and HBCx-19 (*F*). H&E sections, ×200.

their xenografts was established at early and later passages without any observable modifications. The histology of the original tumors was conserved in xenografts. The morphology of cancer cells, the stroma abundance, as well the necrotic areas, *in situ* structures, and surprisingly, inflammatory areas were similarly present in patient tumors and in xenograft biopsies, as determined by optical microscopy. As an example, the original tumor (HBC-13) showed an infiltrating ductal carcinoma (Fig. 1). Note the morphology of cells, very large as typically associated with HER2 overexpression, the necrotic areas, the abundant stroma, and the *in situ* lesions. Histology of the HBCx-13A displayed similar features: large cells, necrotic areas, an abundant stroma of murine origin, and *in situ* tissue morphology. These features were conserved even after several passages. Another example is the tumor HBC-4, a poorly differentiated IDC, and the corresponding xenograft. The third example is the tumor HBC-19, an ILC defined by its morphology and lack of E-cadherin staining (data not shown); HBCx-19 showed the same morphology and the same immunostaining features.

Comparison of cytogenetic features by array-based comparative genomic hybridization. Paired original tumors and xenografted tumors were characterized for genetic parameters using the CGH array technique. They constantly shared the main alterations, but with a lesser number of alterations in the original tumors. This comparison strictly identified xenograft with original tumors; it also showed that genomic rearrangements are at least maintained in xenografts and often accentuated. Complete data will be published separately. One example of array-based comparative genomic hybridization

analysis of the original tumor HBC-13 and its xenograft HBCx-13A is shown in Fig. 2: HBCx-13A had amplifications on chromosomes 8 (8p12, 8q12.1-q12.3) and 17 (17p10, 17q12-q21.2). The xenografted tumors showed the same profile as the original tumors with some additional alterations: amplifications of chromosomes 10 (10q25.1) and 14 (14q12-q13.2, 14q22.1-q22.2), trisomy 7 and monosomy 18. The number of cancer cells in the original tumor was evaluated as >15%, but was mixed with normal human cells, whereas the DNA from the cancer cells in the xenograft was purely human, the stromal cells being murine and the murine DNA does not cross-hybridize with human DNA.

Gene expression profiles. We investigated the status of three suppressor genes (p53, Rb, and PTEN) and of p-AKT and VEGF by Western blotting and that of markers of cell proliferation (Ki67) drug resistance (MDR1, MRP1, MRP5), hormonal receptors (progesterone, estrogen α and β), and tyrosine kinase growth factor receptors (HER1, HER2, HER3, and HER4) by quantitative RT-PCR. HBC xenografts displayed a large diversity of biological profiles (Table 2). Three xenografts had no p53 mutations, whereas 15 xenografts display a p53-mutated status (83%); 6/19 HBCx had no or low Rb expression (30%); 8/19 HBCx did not express PTEN (42%), p-AKT was underexpressed in 7/19 HBCx (37%). PTEN and p-AKT decreases were not correlated. VEGF was detected in 7 HBCx, with high expression in 3 of them. ERα was expressed in two HBCx (HBCx-3 and at the threshold of detection in HBCx-5). mRNA expression of HER1 was elevated in two xenografts, whereas phosphorylated-HER1 (p-HER1) was elevated in 14/18 HBCx (78%); ERBB2 (HER2)-mRNA was high in four xenografts, but amplified only in two of them (HBCx-5 and HBCx-13A/B). HER2 protein was elevated in 50% of HBCx. HER3-mRNA was elevated in HBCx-5 and HBCx-12, and HER4 was low in all xenografts. Ki67 mRNA was high in almost all HBCx. No overexpression of MDR1 was detected, contrasting with MDR1 expression in some original tumors. No overexpression of MRP1 or MRP5 was detected in HBC xenografts (data not shown). A comparison of hormone receptor (ERα and PR) and growth factor receptor (HER) family gene expression was conducted between the nine original tumor samples from patients and their corresponding xenografts (Table 3). Expression of estrogen and progesterone receptors was negative for both patients and xenografts, except for the HBCx-5 tumor xenograft, which showed a slight increase in ERα expression. The expression of HER family genes was globally similar between patients and xenografts, but when the original tumors were positive for HER1 or HER2, expression in the xenografts was equal or superior (HBCx-5 and HBCx-13A). All xenografts but two were highly proliferative as assessed by Ki67 expression.

Growth parameters and drug response of xenografts. A total of 17 HBC xenografts were included in chemotherapeutic assays, and 13 were established before treatment. One was established after docetaxel treatment (HBCx-12A/B) and two were established after anthracycline-based treatment (HBCx-5 and HBCx-7). All xenografts go through an initial phase of tumor regression immediately after transplantation, followed by the reappearance of a palpable tumor and progressive growth. Growth characteristics of HBCx are shown in Table 4. The latency of HBCx (delay between graft and a size of 100 mm^3) was highly variable, with values ranging between 11 and 47 days; their doubling time measured between 250 and 500 mm^3 ranged between 4 and 17 days. These parameters were registered after the third passage in transplantation (between passages 4 and 6) and characterized with few variations from one passage to another. Metastases were detected in the lungs of mice when the tumor mass reached the ethical size before sacrifice. Three xenografts spontaneously

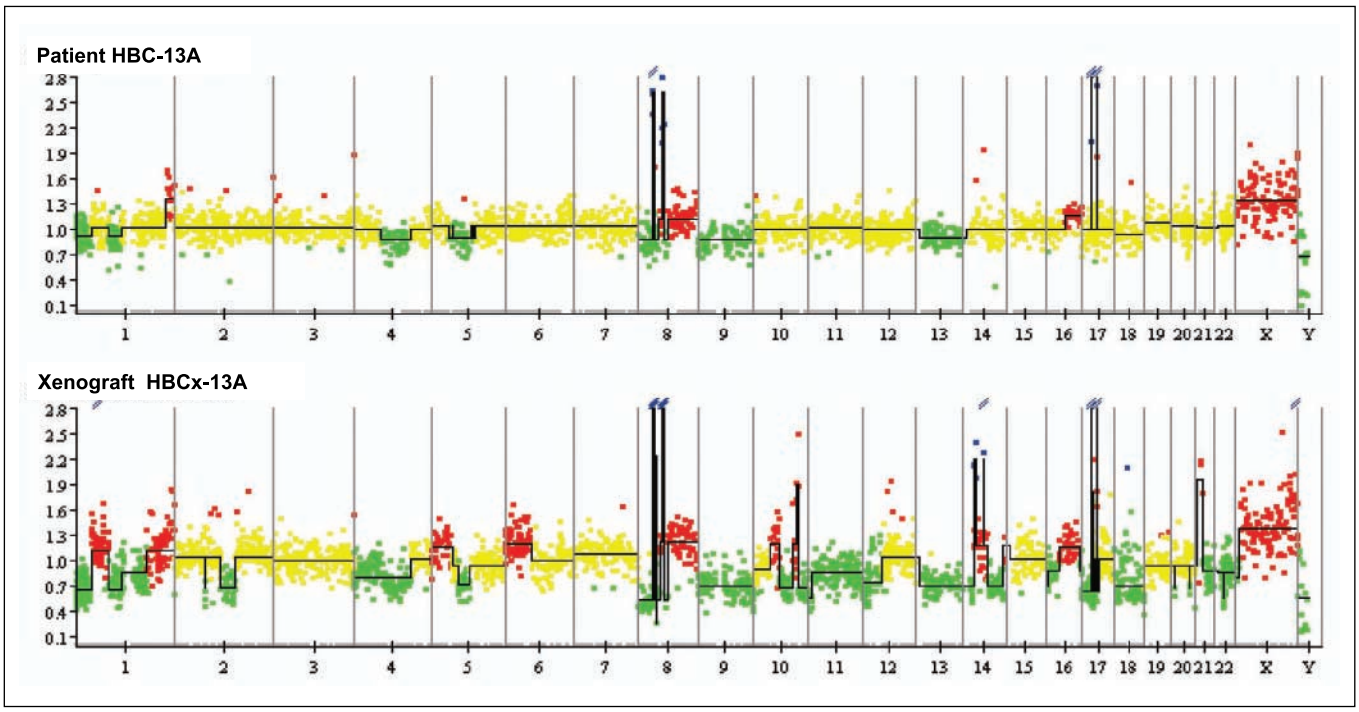

Fig. 2. HBC-13 tumor array CGH profiling of patient (*top*) and xenograft (*bottom*). Loss (*green points*), gain (*red points*), or amplification (*blue points*) of chromosome material, respectively. Recurrence of copy number alterations (*y*-axis) is plotted for each probe aligned along the *x*-axis in chromosome order.

Table 2. Biological characteristics of 21 HBC xenografts originating from 18 patients

Xenograft	Histology	p53	RB*	P-AKT*	PTEN*	VEGF*	ER*	PR	HER1 (mRNA)	p-HER1* (protein)	HER2 (mRNA)	p-HER2* (protein)	HER3	HER4	Ki67
HBCx-1	ICC	Mut	±	±	++	±	78	0	560	+++	**4,416** †	++	310	75	**7,724**
HBCx-2 ‡	ICC	Mut	±	+++	++++	±	0	1	0	++	970	±	46	267	**6,514**
HBCx-3	ICC	Mut	++++	+++	++++	±	**1,381**	16	63	0	563	±	518	708	**5,592**
HBCx-18	ICC	Mut	±	++++	++++	0	0	0	ND	0	ND	0	ND	ND	ND
HBCx-4A	ICC	Mut	++	++++	++++	ND	325	0	**5,221**	+++	460	+++	170	12	**8,046**
HBCx-4B ‡															
HBCx-5§	ICC	WT	+++	+	±	+	**986**	0	1	++++	**78,607**	++++	**2,738**	1,193	**15,326**
HBCx-6	ICC	Mut	++	+++	ND	ND	34	0	1,500	++	1,480	++	192	106	**4,507**
HBCx-7 ‡	ILC	WT	+	0	++	0	0	0	**4,726**	+++	370	±	124	0	**10,861**
HBCx-8	ICC	WT	++++	+	±	0	1	0	648	0	676	+	536	18	**11,528**
HBCx-9	ICC	Mut	±	0	++	+	2	0	1,365	++	1,762	+	1,074	75	**11,484**
HBCx-10	ICC	Mut	±	0	±	0	190	0	673	++	1,622	+	1,119	2	**16,405**
HBCx-11	ICC	Mut	++	0	±	+	0	0	2,195	+++	1,347	++	357	144	**3,509**
HBCx-13A	ICC	Mut	+	+	++++	+++	44	4	320	++++	**30,595**	+++	956	1,468	1,140
HBCx-13B ‡			+	+++	++										
HBCx-14	ICC	Mut	0	0	0	+++	35	0	283	+++	301	+	344	19	**4,158**
HBCx-15	ICC	Mut	+	+	0	+++	15	0	1,080	++	1,056	++	2	0	**5,484**
HBCx-12A§	ICC	Mut	++++	++	±	0	67	1	954	±	5,548	+	**1,960**	45	**7,040**
HBCx-12B ‡ §					0					±		+			
HBCx-19 ‡	ILC	Mut	++	++++	++	0	1	0	ND	+++	ND	++	ND	ND	ND
HBCx-16	ICC	Mut	+++	±	+++	+	1	10	3,138	+++	**7,119**	+	976	124	**7,055**

NOTE: p53 mutations were determined by Fasay Assay. High expression levels are indicated in bold characters.
*Rb, PTEN, P-AKT, p-HER1, HER2 expression (semiquantitative) are by Western blotting analysis; the other genes are by quantitative RT-PCR.
†Overexpression limit, 1,000 units.
‡From metastases, all others from primary tumors.
§Treated before graft.

developed lung metastases with high frequency, (HBCx-12, HBCx-14, HBCx-5), and seven xenografts spontaneously developed lung metastases with low frequency. Lung metastasis histology was clearly similar to the tumor xenograft. A total of 15 of 17 (88%) HBC xenografts responded to the Adriamycin-cyclophosphamide (AC) combination treatments, seven high responders with complete regressions, such as the HBCx-8 (Fig. 3), six were responders, and two were low responders. In these experiments, treatments were not interrupted, and mice were sacrificed after three cycles of 3 weeks treatment plus 10 days. In some cases (HBCx-10 and HBCx-13), mice were observed after the arrest of treatment, and late

Table 3. Comparison between quantitative mRNA expression level of selected genes in nine original tumors and in their corresponding xenografts measured by quantitative RT-PCR

Tumors	ERα	PR	HER1	HER2	HER3	HER4	KI67	Cyclin E1	Cyclin E2
HBC-2*	11	11	158	1,035	138	774	**5,600**	557	4,810
HBCx-2 †	0	1	0	970	46	267	**6,514**	425	5,508
HBC-4	87	7	2,646	551	69	7	**3,105**	569	2,528
HBCx-4	325	0	**5,221**	460	170	12	**8,045**	1,094	5,580
HBC-5	64	3	421	**14,318**	357	108	1,547	473	822
HBCx-5	**986**	0	1	**78,607**	**2,738**	1,193	**15,326**	2,355	**10,614**
HBC-6	6	0	577	671	96	113	**3,972**	982	5,766
HBCx-6	34	0	1,500	1,480	192	106	**4,507**	1,842	5,683
HBC-9	35	23	770	987	358	120	**3,174**	782	2,740
HBCx-9	2	0	1,365	1,762	1,074	75	**11,484**	4,266	**15,412**
HBC-10	207	2	618	1,084	458	1	**15,913**	3,525	4,601
HBCx-10	190	0	673	1,622	1,119	2	**16,405**	3,163	6,111
HBC-13	58	2	151	**20,884**	338	1,435	**2,202**	511	2,362
HBCx-13	44	4	320	**30,595**	956	1,468	1,140	458	5,031
HBC-12	8	18	918	844	737	218	**2,678**	412	1,324
HBCx-12	67	1	954	2,248	1,960	45	**7,040**	537	5,285
HBC-16	26	2	1,179	985	441	90	1,953	570	1,765
HBCx-16	1	10	3,138	**7,119**	976	124	**7,055**	1,730	3,281

NOTE: Numbers in bold correspond to positive or threshold levels of expression.
*Code of patients' tumor.
† Corresponding xenograft.

Table 4. Growth parameters, metastasis occurrence, and drug response of HBC xenografts

Growth parameters				Drug response			
Tumor xenograft code	Doubling time* (days)	Lung metastasis positive/total nb (%)	Treatments	Tumor growth inhibition † (%)	T/C Growth delay index ‡	Complete response (%)	Responder§
HBCx-1	15	1/6	AC	90	No regrowth	100	High R
			Docetaxel	61	2	0	R
HBCx-2	10	1/15 (7%)	AC	18	1.2	0	No
			Docetaxel	18	1.1	0	No
HBCx-3	8	0/20 (0%)	AC	46	1.6	0	No
			Docetaxel	40	1.6	0	No
			Degarelix	60	2.4	0	R
HBCx-4	10	0/11 (0%)	AC	50	1.6	0	No
			Docetaxel	1	1	0	No
HBCx-5	8	15/17 (88%)	AC	90	No regrowth	0	R
			Docetaxel	78	No regrowth	0	R
			Trastuzumab	47	1.1	0	No
HBCx-6	14	0/2	AC	100	No regrowth	100	High R
			Docetaxel	11	1.1	0	No
HBCx-7	9	0/9 (0%)	AC	47	1.4	0	Low R
			Docetaxel	87	No regrowth	25	R
HBCx-8	5	3/29 (10%)	AC	100	No regrowth	100	High R
			Docetaxel	42	1.6	0	Low R
HBCx-9	5	0/23 (0%)	AC	68	No regrowth	0	R
			Docetaxel	100	No regrowth	25	R
HBCx-10	17	1/19 (5%)	AC	100	No regrowth	100	High R
			Docetaxel	48	1.1	0	No
HBCx-11	14	1/4	AC	85	No regrowth	0	R
			Docetaxel	48	1.7	0	Low R
HBCx-13	13	3/14 (21%)	AC	100	No regrowth	100	High R
			Docetaxel	46	1.05	0	No
			Trastuzumab	95	No regrowth	100	High R
HBCx-14	10	7/8 (88%)	AC	80	No regrowth	0	R
			Docetaxel	23	1.7	0	No
HBCx-15	4	0/23 (0%)	AC	99	No regrowth	100	R
			Docetaxel	42	1.4	0	No
HBCx-12	7	16/16 (100%)	AC	52	2	0	R
			Docetaxel	28	1	0	No
HBCx-16	17	1/2	AC	73	No regrowth	0	R
			Docetaxel	19	1	0	No
HBCx-17	12	0/3	AC	100	No regrowth	100	High R
			Docetaxel	42	1.2	0	No

Abbreviation: AC, Adriamycin-cyclophosphamide combination.
*Time in days required to double the tumor size, during the exponential phase of growth.
† TGI (tumor growth inhibition) is the optimal ratio between the mean tumor volume in the treated group and that in the control group × 100, at the same time.
‡ T/C growth delay index is the ratio between the survival of treated mice and the survival of control mice. This index cannot be calculated in case of complete response.
§ Four categories of HBCx responders (*R*) were defined as detailed in Materials and Methods: (*a*) high R, (*b*) responders (R), (*c*) Low R, and (*d*) the nonresponders (*Not in the tables*).

recurrences could be observed. A total of 8 of 17 HBCx (47%) responded to docetaxel treatment, with few complete regressions, but frequent lack of regrowth under treatment, as shown for HBCx-7, in Fig. 3. Four of the eight were low responders. A significant tumor growth inhibition was obtained by the administration of trastuzumab (weekly for 2 months) to mice bearing ERBB2 (HER2)-amplified HBC. The response of HBCx-5 did not reach the defined threshold for a response. HBCx-13 responded well with the induction of complete regressions. No response was seen in three HBCs that did not overexpress ERBB2 (HER2). Coadministration of trastuzumab with docetaxel induced additive effects with HBCx-5 with a significant benefit (data not shown). Hormone deprivation induced by Degarelix, a Gonadotropin-releasing hormone (GnRH) antagonist, reduced the growth of HBCx-3, the ER-positive HBC.

Comparison of drug response in patients and in the corresponding tumor xenografts. A concordance between the response of original tumors in the patients and the chemosensitivity of their corresponding xenografts was looked for. Such an analysis was possible only in cases in which the same treatment was administered in patients and in xenografts. However, in case of adjuvant treatment in the clinical setting, a response cannot be meaningfully assessed. Therefore, concordance was established in only seven cases. Objective responses to treatment were documented by clinicians according to WHO criteria and are summarized in Table 5. A clinical progression was observed after neoadjuvant therapy, concordant with the resistance of the xenograft. In 45 cases of first or second line of treatment, patient tumors relapsed or progressed, and lack of response was observed in two of the four xenografts. In two cases

of response to the first-line treatment, a response was observed with the xenograft. Among the clinical cases, two were responses and were concordant with xenograft sensitivity. Five clinical cases concerned relapses or progression, three were concordant with lack of response of xenografts. The overall concordance was 5/7.

Discussion

The aim of this work was to establish a panel of xenografts of HBC transplantable into immunocompromised nude mice. Such a panel of breast cancer xenografts might be the closest model to human cancers currently available. These preclinical models could help to test the efficacy of new antitumor drugs or new combinations and would seem to improve the predictive potential of preclinical assays. The panel of HBC xenografts comprises a selection of aggressive tumors, with a majority of triple-negative tumors. Triple-negative tumors have the worst prognosis, recurring frequently after treatment, and they are candidates for chemotherapies. Although we grafted a large number of ER-positive breast cancers, only 4% took in mice, and when they did it, almost all were lost before the third passage. HBCx-3 was the unique ER-positive xenograft which was established. Therefore, although the panel reflects a strong selection bias toward aggressive tumors, disease heterogeneity persists in terms of histology and biological parameters.

Among the large variety of tumors transplantable into immunodeficient mice, breast cancers seem to be very difficult to establish (2, 3). Different reasons can explain this low tumor take, as follows: (*a*) The genetic background of the recipient mice. Experience of other authors suggests that using more profoundly immunodeficient mice could enhance the tumor take (10, 11). (*b*) The choice of site of implantation. Our experience shows that the interscapular fat pad provides higher tumor take than orthotopic sites: using double implantation (mammary fat pad and interscapular area) in the same mouse, we observed differences of tumor engraftment in favor for the interscapular fat pad.[7] Implantation in the renal capsule might be susceptible to promote growth as a result of the rich vascularity (12) and could lead to an increase in the take especially of low-grade ER-positive tumors, which are very difficult to maintain in serial passages. (*c*) The hormone status of breast tumors is a critical parameter: ER-negative tumors show a significant superiority of tumor take when compared with ER-positive tumors. ER-positive HBC have slow-growing properties (13), a low grade, or slow proliferation (14). Our failure to establish more ER-positive HBCx is in accordance with data reported by the Fribourg group (1) and other authors (15), who showed that ER-negative tumors were easier to establish in mice. The weak tumor take could also be attributed to differences between the hormonal status of female mice and women. Although we provided estrogens to mice during tumor take and growth, this supply could either be insufficient or simply inappropriate. The tumor take rate was better when the biopsy came from a metastasis. However, engraftment of tumor tissue from primary sites of metastatic tumors was not higher than that of primary sites of nonmetastatic tumors. Adaptation of the tumor cells to the ectopic environment of another organ seemed to favor the tumor take in a xenogenic environment. Globally, aggressiveness of the engrafted tissue influenced the frequency of tumor take in our assays, as also observed by Sharkey et al. (16).

The majority of xenografts were infiltrating ductal carcinomas, with 18% rate of tumor take; lobular carcinomas showed a lower tumor take (8%). These findings are consistent with the report of Giovanella et al. (17). The *in situ* morphology, which is frequently associated with infiltrating carcinoma, did not reduce tumor take, and xenografts maintained this original feature. Tumor take rate was correlated with the high grade of tumors, as expected, but not with lymph node involvement, which is more surprising.

It is well known that s.c. transplanted human tumors rarely develop metastases in nude mice, which are a crucial target of anticancer drugs. In our series of models, about a third of xenografts developed lung metastases, and three HBCx were consistently metastatic. With the exception of a human tumor breast line reported by Hurst et al. (18), this is the first panel of human breast tumor xenografts developing spontaneously metastasis in the lung. It is noticeable that metastatic xenografts originated from invading tumors in patients. We did not search for metastatic foci in other sites, such as bone marrow or skeleton. The majority of our HBC xenografts displayed a mutated p53, whereas the overall frequency of p53 mutations in breast carcinomas is about 20% to 40% depending on stage (19). This indicates a selection bias to mutated p53 tumors through engraftment into nude mice. This was reported in ovarian cancer, where abnormal p53 expression was associated

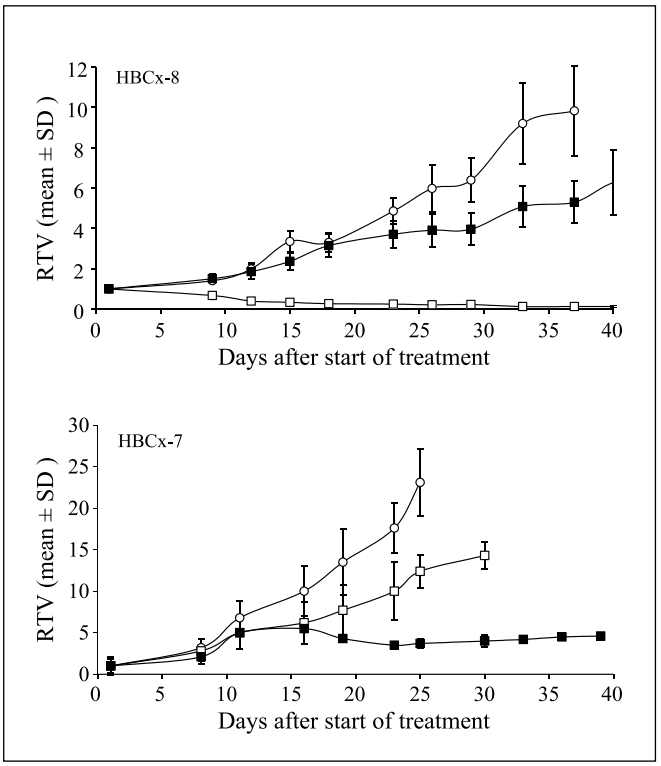

Fig. 3. Tumor growth curves of HBCx-8 and HBCx-7 xenografts as a function of time: HBCx-8 bearing mice (*top*) and HBCx-7 tumor (*bottom*) were treated with two cycles of AC (□), a combination of doxorubicin (2 mg/kg) and of cyclophosphamide (100 mg/kg) or with docetaxel (■; 20 mg/kg, i.p. every 3 wks). Controls (○) were not treated. Mice were treated at day 1, and tumor volume was measured twice a week. Tumor growth was evaluated by plotting the mean of the RTV (relative tumor volume) ± SD per group (each group consisted of 10 mice) over time after first treatment.

Table 5. Relationship between patients' clinical responses and the chemosensitivity of the corresponding xenografts

Tumor code	Compound	Phase of therapy	Clinical response	Response of the xenograft	Concordance
HBC-12	Docetaxel	Neoadjuvant	Progression	No response	Yes
HBC-1	Docetaxel	First line	Partial response	Response	Yes
HBC-3	Docetaxel/5FU	First line	Stable disease	Low response	Yes
HBC-5	Docetaxel	First line	Progression	Response	No
HBC-9	Docetaxel	First line	Progression	Response	No
HBC-15	Docetaxel	First line	Progression	No response	Yes
HBC-5	Trastuzumab	Second line	Progression	No response	Yes

with tumorigenicity in nude mice (20). Conversely, no correlation was found in our models between tumor take rate and ERBB2 (HER2) overexpression or amplification, as reported by Giovanella et al. (17). Expression levels of genes involved in proliferation and death regulators like p53, Rb, VEGF, PTEN, and p-AKT showed marked heterogeneity. Among growth factors, VEGF has been shown to play a role in breast carcinoma, as higher levels of cytosolic VEGF are a strong predictor of relapse-free survival and overall survival in primary node-positive breast cancer after adjuvant treatment (21).

p-AKT expression level was variable from very high to null. It was not correlated with the loss of PTEN expression, which was found in 42% of HBCx. Some reports indicated that p-AKT expression was inversely correlated with that of PTEN. However, a recent study conducted on more than 600 primary operable breast cancers provided evidence against the current model of a simple linear tumorigenic PTEN – phosphoinositide-3-kinase – AKT – mTOR pathway in breast cancer and indicated that loss of PTEN expression is not frequent in breast cancers (22). Histology of the patient's tumors was compared with that of the xenografted tumors; the majority of xenografts had the same characteristics of the original tumors, the same histologic type, and the same differentiation even after several passages. Importantly, the *in situ* architecture was inherited by the xenografts. The stroma content was reconstituted in the xenografts, with an abundance similar to that of the original tumor. This is quite surprising because the xenograft stroma is of murine origin, indicating that interactions between the human tumor cells and the host are similarly active *in vivo* in humans and mice. Stromal fibroblasts and host cells produce paracrine factors that have a profound influence on the growth of cancer cells, metastatic spread, and pharmacologic response (23).

Comparison of the biological profile of the original tumors and their xenografts was possible in nine cases. Gene expression profile of the HER family, Ki67, and cyclins was similar between paired tumors. In a few cases, gene expression was more pronounced in xenografts than in patients probably because the patient tumor is more heterogeneous due to the content of normal stroma.

The genetic relationship between xenografts and the corresponding patient tumors was established by array-based CGH; alterations specific to each xenograft and original tumor will be described in detail elsewhere.[8] Genetic alterations were globally found to be similar, but in some cases, amplifications or deletions of the same loci were more accentuated in the xenograft than in the corresponding patient tumor. For example, HBCx-3 xenograft displayed more gene amplifications than its original counterpart, whereas HBCx-10 or HBCx-13 profiles were very close to those of the patient tumors. These differences could partially be explained by the presence of native human DNA in the original tumors. The human xenograft DNA is purely tumoral because the connective tissue present in the xenograft is murine and had no cross-hybridization with human DNA. This could explain small-amplitude alterations, but cannot account for some other alterations present in the xenograft and not seen in the original tumor. It could be postulated that the transplantation can lead, in some cases, to selection of more aggressive tumor cell subpopulations. The biological profile of the whole HBCx panel indicates that engraftment into immunocompromised mice selects for triple-negative HBCx (negative for ER, PR, and HER2), including basal-like subtype HBCx. The basal-like subtype is an aggressive type of breast cancer (24, 25). A review by Brenton (26) also highlighted the aggressiveness of the triple-negative subtype of HBC. Triple-negative HBCx represents 15% of breast cancers and is the most aggressive, with the highest frequency of recurrences.

Three HBCx expressed biological markers, allowing categorization into different subtypes: HBCx-3 was ER positive, HBCx-13A and HBCx-5 were HER2 positive. In addition to expression of ER, HBCx-3 displayed markers of aggressiveness, such as negative PR and mutated p53. HBCx-13A/B and HBCx-5 shared overexpression and amplification of ERBB2 (HER2), but differed in other important parameters: HBCx-13A/B having a mutated p53, but a functional PTEN and a deficient Rb; whereas HBCx-5 had a wt p53, but a loss of function of PTEN and a functional Rb.

Responses of HBC xenografts to anthracycline-based therapy (AC) or to docetaxel tested in the same experimental conditions can be compared. Only one HBCx did not respond to any chemotherapy (HBCx-2). A total of 14 of 17 responded to AC (88%), and 8 responded to docetaxel (48%). This indicates that triple-negative HBCx respond more frequently to anthracycline-based therapy than to docetaxel. Response to trastuzumab was observed in only one of the two HBCx, both overexpressed HER2 associated with gene amplification. Synergistic interactions of trastuzumab plus docetaxel were also observed in both ERBB2 (HER2)-overexpressing HBC xenografts (data not shown), as observed in cell lines *in vitro* and *in vivo*, indicating that the combination of docetaxel plus trastuzumab has better antitumor efficacy than either agent alone (27, 28).

No relationship was found between chemosensitivity and the biological profile of the xenografts, likely due to their limited

[8] In preparation.

number, or alternatively to the limited number of biological markers studied. The absence of expression of chemoresistance-associated genes like MDR1, MRP1, and MRP5 in our xenografts could explain the high frequency of response to AC in our models. Alternatively, the high frequency of response to anthracycline-based therapy could be related to the high frequency of mutated p53. These findings are in agreement with some reports indicating that p53 mutated xenografts are more resistant than p53 wild-type xenografts to mitomycin C, cisplatin, or radiotherapy, but not to doxorubicin or cyclophosphamide (29, 30).

The response of HBCx-3 to hormone deprivation was tested using Degarelix, a powerful antagonist of GnRH, which is highly effective in the treatment of prostate cancer (4). This compound inhibits HBCx-3 growth.

As first shown by the Freiburg group (31) in several histologic models, tumor xenograft drug response was highly correlated with the clinical outcome of patients; the drug response of xenograft models correctly predicted response in 90% (19 of 21 tumors) and resistance in 97% of the patients (57 of 59 tumors).

Our own data must be cautiously interpreted, due to the small number of cases and to the heterogeneity of treatments. Strictly, a response to treatment could be determined only in a neoadjuvant and metastatic setting; a concordance was found in 5/7 analyzable cases. For four other patients treated in an adjuvant setting, response to chemotherapy could not be precisely assessed; a relapse within 6 months after the end of treatment may reflect resistance to therapy, but also failure of local treatment. Nevertheless, a concordance between the outcomes of these patients with the drug response of xenografts was found in all cases.

In conclusion, the present work describes a large panel of breast tumor xenografts, representative of aggressive HBC and of their biological heterogeneity. The majority of tumors were triple-negative, for which there is a clinical need to develop new therapies because they are not candidates for targeted therapy (hormone therapy and trastuzumab, for example). Preliminary results of concordance between clinical outcome and response of xenografts support the use of human tumor xenografts for the preclinical evaluation of new compounds targeting breast cancer and predicting response to treatment.

Acknowledgments

Dr. Christophe Rosty (Institut Curie, Paris) and Pr. Hughes deThé, (Hopital Saint-Louis, Paris) for their helpful contribution, Catherine Barbaroux, Vincent Bordier (Institut Curie, Paris), and Louis-François Plassa, (Hopital Saint-Louis, Paris) for their technical assistance. La Ligue Contre le Cancer for its support to the array-based comparative genomic hybridization platform.

References

1. Boven E, Winograd B, Berger DP, et al. Phase II preclinical drug screening in human tumor xenografts: a first European multicenter collaborative study. Cancer Res 1992;52:5940–7.
2. Fiebig HH, Burger AM. Human tumor xenografts and explants. In: Teicher BA, editor. Tumor models in cancer research. Totowa (NJ): Humana Press; 2001. p. 113–7.
3. Mattern J, Bak M, Hahn EW, Volm M. Human tumor xenografts as model for drug testing. Cancer Metastasis Rev 1988;7:263–84.
4. de Pinieux G, Legrier ME, Poirson-Bichat F, et al. Clinical and experimental progression of a new model of human prostate cancer and therapeutic approach. Am J Pathol 2001;159:753–64.
5. Flaman JM, Robert V, Lenglet S, Moreau V, Iggo R, Frebourg T. Identification of human p53 mutations with differential effects on the bax and p21 promoters using functional assays in yeast. Oncogene 1998;16:1369–72.
6. Waridel F, Iggo R. Identification of clonal mutations in morphologically normal mucosa of the aerodigestive tract. Eur J Cancer Prev 1996;5:67–73.
7. de Cremoux P, Bieche I, Tran-Perennou C, et al. Inter-laboratory quality control for hormone-dependent gene expression in human breast tumors using real-time reverse transcription-polymerase chain reaction. Endocr Relat Cancer 2004;11:489–95.
8. de Cremoux P, Jourdan-Da-Silva N, Couturier J, et al. Role of chemotherapy resistance genes in outcome of neuroblastoma. Pediatr Blood Cancer 2007;48:311–7.
9. Brisset S, Schleiermacher G, Peter M, et al. CGH analysis of secondary genetic changes in Ewing tumors: correlation with metastatic disease in a series of 43 cases. Cancer Genet Cytogenet 2001;130:57–61.
10. Visonneau S, Cesano A, Torosian MH, Miller EJ, Santoli D. Growth characteristics and metastatic properties of human breast cancer xenografts in immunodeficient mice. Am J Pathol 1998;152:1299–311.
11. Clarke R. Animal models of breast cancer: their diversity and role in biomedical research. Breast Cancer Res Treat 1996;39:1–6.
12. Fingert HJ, Chen Z, Mizrahi N, Gajewski WH, Bamberg MP, Kradin RL. Rapid growth of human cancer cells in a mouse model with fibrin clot subrenal capsule assay. Cancer Res 1987;47:3824–9.
13. Hoehn W, Schroeder FH, Reimann JF, Joebsis AC, Hermanek P. Human prostatic adenocarcinoma: some characteristics of a serially transplantable line in nude mice (PC 82). Prostate 1980;1:95–104.
14. Daidone MG, Coradini D, Martelli G, Veneroni S. Primary breast cancer in elderly women: biological profile and relation with clinical outcome. Crit Rev Oncol Hematol 2003;45:313–25.
15. Bailey MJ, Gazet JC, Peckham MJ, Human breast-cancer xenografts in immune-suppressed mice. Br J Cancer 1980;42:524–9.
16. Sharkey FE, Fogh J. Considerations in the use of nude mice for cancer research. Cancer Metastasis Rev 1984;3:341–60.
17. Giovanella BC, Vardeman DM, Williams LJ, et al. Heterotransplantation of human breast carcinomas in nude mice. Correlation between successful heterotransplants, poor prognosis and amplification of the HER-2/neu oncogene. Int J Cancer 1991;47:66–71.
18. Hurst J, Maniar N, Tombarkiewicz J, et al. A novel model of a metastatic human breast tumour xenograft line. Br J Cancer 1993;68:274–6.
19. Borresen-Dale AL. TP53 and breast cancer. Hum Mutat 2003;21:292–300.
20. Verschraegen CF, Hu W, Du Y, et al. Establishment and characterization of cancer cell cultures and xenografts derived from primary or metastatic Mullerian cancers. Clin Cancer Res 2003;9:845–52.
21. Linderholm B, Tavelin B, Grankvist K, Henriksson R. Vascular endothelial growth factor is of high prognostic value in node-negative breast carcinoma. J Clin Oncol 1998;16:3121–8.
22. Panigrahi AR, Pinder SE, Chan SY, Paish EC, Robertson JF, Ellis IO. The role of PTEN and its signalling pathways, including AKT, in breast cancer; an assessment of relationships with other prognostic factors and with outcome. J Pathol 2004;204:93–100.
23. Bhowmick NA, Neilson EG, Moses HL. Stromal fibroblasts in cancer initiation and progression. Nature 2004;432:332–7.
24. Sorlie T. Molecular portraits of breast cancer: tumour subtypes as distinct disease entities. Eur J Cancer 2004;40:2667–75.
25. Bryan BB, Schnitt SJ, Collins LC. Ductal carcinoma *in situ* with basal-like phenotype: a possible precursor to invasive basal-like breast cancer. Mod Pathol 2006;19:617–21.
26. Brenton JD, Carey LA, Ahmed AA, Caldas C. Molecular classification and molecular forecasting of breast cancer: ready for clinical application? J Clin Oncol 2005;23:7350–60.
27. Pegram MD, Konecny GE, O'Callaghan C, Beryt M, Pietras R, Slamon DJ. Rational combinations of trastuzumab with chemotherapeutic drugs used in the treatment of breast cancer. J Natl Cancer Inst 2004;96:739–49.
28. Merlin JL, Barberi-Heyob M, Bachmann N. *In vitro* comparative evaluation of trastuzumab (Herceptin) combined with paclitaxel (Taxol) or docetaxel (Taxotere) in HER2-expressing human breast cancer cell lines. Ann Oncol 2002;13:1743–8.
29. Kolberg HC, Villena-Heinsen C, Deml MM, Kraemer S, Diedrich K, Friedrich M. Relationship between chemotherapy with paclitaxel, cisplatin, vinorelbine and titanocene dichloride and expression of proliferation markers and tumour suppressor gene p53 in human ovarian cancer xenografts in nude mice. Eur J Gynaecol Oncol 2005;26:398–402.
30. Henriksson E, Baldetorp B, Borg A, et al. p53 mutation and cyclin D1 amplification correlate with cisplatin sensitivity in xenografted human squamous cell carcinomas from head and neck. Acta Oncol 2006;45:300–5.
31. Fiebig HH, Maier A, Burger AM. Clonogenic assay with established human tumour xenografts: correlation of *in vitro* to *in vivo* activity as a basis for anticancer drug discovery. Eur J Cancer 2004;40:802–20.

Clinical Cancer Research

A New Model of Patient Tumor-Derived Breast Cancer Xenografts for Preclinical Assays

Elisabetta Marangoni, Anne Vincent-Salomon, Nathalie Auger, et al.

Clin Cancer Res 2007;13:3989-3998.